Structure of Poly(ferrocenyldimethylsilane) in Electrospun Nanofibers

5 **AUTHORS**, INCLUDING:

Mark D. Foster
University of Akron
195 PUBLICATIONS **2,488** CITATIONS

SEE PROFILE

Hao Fong
South Dakota School of Mines and Technology
125 PUBLICATIONS **4,998** CITATIONS

SEE PROFILE

Structure of Poly(ferrocenyldimethylsilane) in Electrospun Nanofibers

Zhihao Chen, Mark D. Foster,* Wensheng Zhou, Hao Fong, and Darrell H. Reneker

Department of Polymer Science, The University of Akron, Akron, Ohio 44325

Rui Resendes and Ian Manners

Department of Chemistry, University of Toronto, 80 St. George Street, Toronto, Ontario M5S 3H6, Canada

Introduction. Poly(ferrocenylsilane) polymers, consisting of alternating ferrocene units and silicon atoms in the main chain, have novel redox, electrical, optical, chemical, and other characteristics.[1−3] Replacing the conventional condensation synthesis by ring-opening polymerization (ROP) of silicon-bridged ferrocenophane has made it possible to make well-defined, high molecular weight materials and to tailor their structure.[4−6] These materials present scientific challenges both in characterizing their structure and in understanding how this structure can best be exploited in various applications.

Poly(ferrocenyldimethylsilane), $\{-[fc-Si(CH_3)_2-]_n-$, where $fc = Fe(\eta\text{-}C_5H_4)_2\}$ is a recently discovered crystalline material. Single crystals obtained by precipitation from solution of the pentamer analogue, penta(ferrocenyldimethylsilane),[7] have been characterized with wide-angle X-ray diffraction (WAXD). Those X-ray diffraction data displayed many sharp peaks,[7] with the most intense corresponding to d spacings of 0.58, 0.63, and 0.66 nm. The investigators in that work proposed a triclinic crystal structure[7] having the lattice parameter values $a = 1.176$ nm, $b = 1.185$ nm, $c = 1.251$ nm, $\alpha = 94.85°$, $\beta = 114.15°$, and $\gamma = 117.66°$. Powder patterns of poly(ferrocenyldimethylsilane) (PFDMS) polymers[8] (Figure 1) of several molecular weights have also been measured. The WAXD data showed the strongest peak at a d spacing of 0.637 nm. The authors ascribed that spacing to the distance between sets of planes containing the iron atoms since that element has a relatively high scattering length. Other peaks seen in the WAXD pattern from each polymer powder were associated with d spacings of 0.379, 0.445, and 1.106 nm.[8]

One form into which the poly(ferrocenylsilane) polymers could be processed to provide novel possibilities is that of nanofibers.[9,10] Nanofibers created by electrospinning[11,12] have very high surface area to mass ratios, e.g., 1000 m²/g for a fiber with a diameter of 50 nm. The smallest nanofibers[13] with a diameter of only 3 nm have 50% of the molecules on the surface. They present a confined environment in which one might expect deviations in the structure from that characteristic of conventional fibers. Here electron diffraction from a segment of a single nanofiber has been used to characterize its crystalline structure, which is compared with what is known of the crystal structure in related samples. Unit cell parameters were determined using usual methods for analysis of X-ray fiber diffraction patterns.

Experimental Section. The poly(ferrocenyldimethylsilane) homopolymer used to create nanofibers was
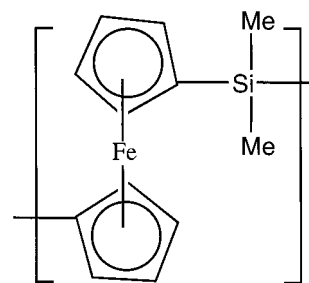

Figure 1. Chemical structure of poly(ferrocenyldimethylsilane).

prepared by Pt-catalyzed ROP in the presence of Et_3SiH[1] and had a molar mass, M_w, of 87 000 g/mol and polydispersity index of 1.3 as measured by gel permeation chromatography using universal calibration relative to polystyrene standards. The polymer powder was dissolved at room temperature in a mixture of 90 wt % tetrahydrofuran and 10 wt % dimethylformamide to create a viscous orange solution that contained 30 wt % polymer.

PFDMS nanofibers were created by electrospinning. The setup of the apparatus has been described elsewhere.[12] The solution was first transferred into a capillary pipet charged to a high electrical potential (160 μA at 30 kV). As the electrical potential was gradually increased, a liquid jet issued from the surface of the droplet and flew toward a grounded metal mesh collector. The solidified nanofibers were collected on a grid for study with transmission electron microscopy (TEM) or on a screen or cover glass for study by optical microscopy and scanning electron microscopy (SEM). A layer of evaporated carbon was deposited on the TEM sample grids to prevent the nanofibers from becoming charged by the electron beam.

A Nikon polarizing microscope was used to observe and photograph the nanofibers on cover glasses. The morphology of fibers and distribution of fiber sizes were observed using SEM. Smaller scale morphology was observed using a JEOL JEM-1200IIX microscope operated at an accelerating voltage of 120 kV. Electron diffraction patterns were recorded on photographic film and scanned using a digital image scanner (Minolta Dimage Scan Multi Scanner).

Results and Discussion. The fibers studied ranged from around 100 to 1000 nm in diameter. When observing a collection of nanofibers with different diameters, using backscattered light (epi-illumination with white light) by optical microscopy, different interference colors were seen from fibers of different diameter. Birefringence characteristic of fibers with polymer molecules extended along the fiber axis was observed by rotating the fibers between crossed polarizers in an optical microscope.

A TEM negative image (150 000×) of a short segment of one nanofiber is shown in Figure 2. The variation in brightness across the fiber reveals that the beam is able to penetrate the fiber and that the distance traversed by the beam varies from the edge of the fiber to the middle. Figure 3a presents an electron diffraction pattern from the as-spun nanofiber shown in Figure 2 taken with the fiber axis perpendicular to the electron beam. The pattern is consistent with the notion that

Figure 2. TEM image (negative) of a 150 nm diameter poly-(ferrocenyldimethylsilane) nanofiber.

the polymer chains are extended and aligned along the fiber axis. Diffraction peaks are observed on the meridian on the second, fourth, and eighth layer lines. A d spacing of 0.634 ± 0.8 nm for the (002) spot on the meridian indicates a value of 1.27 nm for the c-axis lattice parameter. The 0.634 nm d spacing agrees well with the spacing corresponding to the dominant reflection in the powder patterns both from exactly the same polymer[14] and from other PFDMS polymers of identical chemical composition, but different molecular weight.[5,7] The strong diffraction peak on the equator in Figure 3a corresponds to a d spacing of 0.58 nm. A similar spacing is seen in the WAXD data from the pentamer single crystals[7] and also in a WAXD powder pattern from a PFDMS polymer studied by Nguyen and co-workers.[5] The diffraction pattern from the nanofiber indicates a simple 2/1 screw symmetry and the $c*$ axis is perpendicular to the $a*b*$ plane, which eliminates the possibility of a triclinic cell such as that reported[7] for the crystal structure of the pentamer. Weak diffraction spots are observable in each quadrant at the third layer line in the negative reproduced in Figure 3a.

After annealing the nanofibers at 75 °C, which is about 40 deg above the glass transition temperature of PFDMS and well below the melting temperature, for 6 h, the sharper diffraction pattern shown in Figure 3b was observed. There are many spots present on the negative that could not be captured in the scanned image, due to the large dynamic range required. Therefore, a hand-drawn enlargement of a portion of the diffraction pattern is presented in Figure 3c. The pattern was reproduced by making precise measurements from the negative using a Nikon comparator. The d spacings corresponding to the equatorial spots are recorded in Table 1 and compared with values from X-ray diffraction measurements, by others, of the pentamer model compound[8] and two PFDMS polymers of high molecular weight.[15] (Reference 15 appeared while this contribution was in revision.) The strong diffraction peak on the equator for d around 0.58 nm remains after annealing. Additional diffraction spots appeared on the equator after annealing. By determining the d spacings of all ($hk0$) spots on the equator, constructing a basic triangle to expand the lattice in the $a*b*$ plane, and
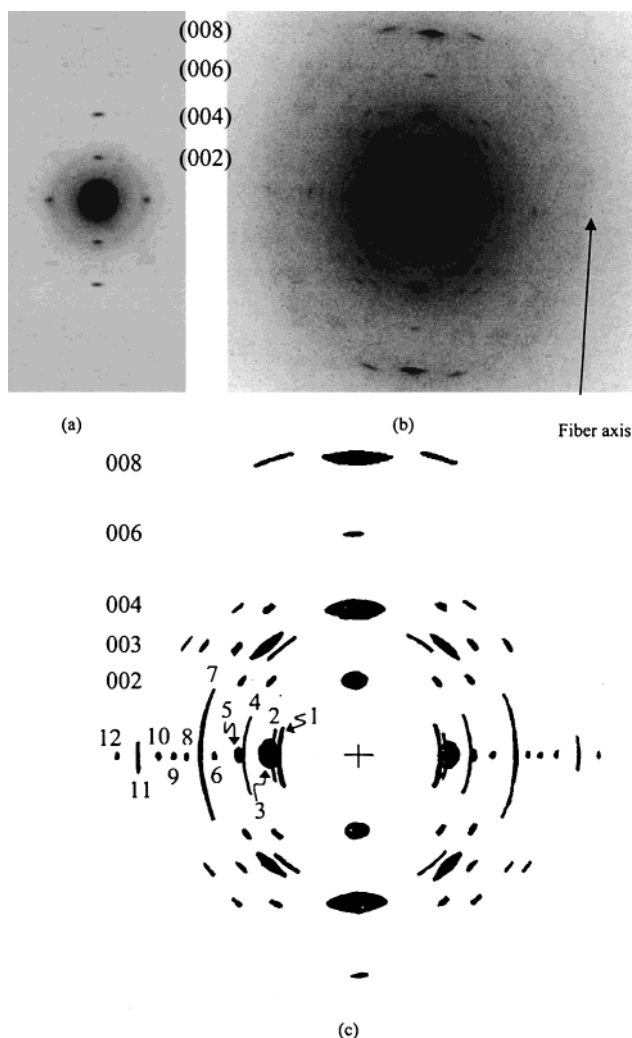

Figure 3. (a) Low-dose electron diffraction pattern from an as-spun nanofiber with the electron beam perpendicular to the fiber axis. (b) Electron diffraction pattern from a nanofiber after being annealed at 75 °C for 6 h. The (0010) meridional spots are also clearly observable in the negative but have been cropped from this image to allow enlargement of the central portion of the pattern. (c) Traced pattern for a portion of (b). The (008) layer line at the bottom has been omitted for clarity.

matching each diffraction spot with a lattice point, we concluded that the PFDMS molecules adopt a monoclinic unit cell in the nanofibers. The arcs labeled 1, 4, 7, and 11 in Figure 3c were not included in the unit cell determination as they are of an interesting and different character than the other equatorial reflections. The final refinement was based on 22 reflections, including those in the quadrants. The unit cell parameters so determined were $a = 1.42$ nm, $b = 0.603$ nm, $c = 1.39$ nm, and $\gamma = 95.1°$. These values correspond to a crystallographic density of 1.35 g/cm^3.

Two tilting experiments were also performed. The fiber was first rotated about its axis. The diffraction pattern did not change. This finding supports the view that even in a fiber with a diameter as small as 150 nm, there are a large number of crystallites. Consider the intensity of an equatorial diffraction spot, for example that from (020) planes. If there were only a few crystallites in the fiber, this diffraction spot for each crystallite would be intense when the Bragg condition was satisfied for one of the crystallites and weak at other angles. If at some angles no crystallite would

Table 1. Comparison of *d* spacings (nm) of Equatorial Spots/Arcs from Different Works

feature label	this work[a]	pentamer[b]	polymer Manners[c]	polymer Pannell[d]
				1.106 (w)
		0.902 (s)		
e	0.713	0.660 (s)		
				0.663 (w)
1	0.636 (s)	0.632 (vs)	0.637 (vs)	
2	0.599 (w)	0.590 (s)		0.60 (s)
3	**0.583 (s)**			
		0.562 (w)		0.560 (w)
		0.530 (s)		0.532 (w)
		0.521 (w)		
		0.499 (w)		
		0.487 (w)		
4	0.444 (w)	0.450 (w)	0.445 (s)	0.443 (vw)
5	**0.436 (w)**			
		0.413 (w)		
		0.399 (w)		
		0.388 (w)		
		0.382 (w)	0.379 (s)	
		0.363 (w)		
6	**0.354 (w)**	0.353 (w)		
		0.340 (w)		
7	0.322 (w)	0.324 (w)		
		0.310 (w)		
8	**0.299 (w)**	0.292 (w)		
		0.285 (w)		
9	**0.279 (w)**			
10	0.259 (w)			
11	0.230 (w)			
12	**0.212 (w)**			

[a] vs = very strong, s = strong, w = weak, vw = very weak. In this column bold figures denote spots; others are arcs. [b] Reference 8. [c] Reference 8. Solid-state polymerized, M_w = 260 000, M_w/M_n = 1.5. [d] Reference 15. M_w = 116 000, M_w/M_n = 2.1. [e] Borrowed from third layer.

satisfy the Bragg condition, the intensity of an equatorial spot would change during rotation. An uniform intensity of the (020) diffraction spots during rotation of the sample suggests that there are so many crystallites, with random azimuthal orientations, that about the same number of crystallites satisfies the Bragg condition, whatever the azimuth of the incident X-ray beam.

The fiber was also tilted about an axis perpendicular to both the fiber axis and the electron beam at monotonically increasing angles of 8, 16, 28, 38, and 45°. As the tilting angle increased, the diffraction spots on the meridian disappeared as all the *00l* lattice points were rotated away from the Bragg condition, while the strong diffractions on the equator remained. The diffraction spots on the third layer also moved toward the meridian.

Summary. The novel organometallic polymer poly-(ferrocenyldimethylsilane) can successfully be formed into nanofibers by electrospinning and the crystal structure of the polymer in these unusually thin fibers studied using electron diffraction on single fibers. The chains (and crystals) are oriented along the fiber axis. The *c*-axes of the crystals are along the fiber axis, but both *a*- and *b*-axes of a multitude of crystals are randomly distributed in the azimuthal directions. The data are consistent with the assignment of a monoclinic unit cell for the crystals in the nanofiber, which is different from the triclinic structure observed for pentamer single crystals.

References and Notes

(1) Manners, I. *Chem. Commun.* **1999**, 857.
(2) Manners, I. *Adv. Organomet. Chem.* **1995**, *37*, 131.
(3) Hmyene, M.; Yassar, A.; Escorne, M.; Percheron-Guegan, A.; Garnier, F. *Adv. Mater.* **1994**, *6*, 564.
(4) Rulkens, R.; Ni, Y.; Manners, I. *J. Am. Chem. Soc.* **1994**, *116*, 12121.
(5) Nguyen, M. T.; Diaz, A. F.; Dement'ev, V. V.; Pannell, K. H. *Chem. Mater.* **1993**, *5*, 1389.
(6) Pudleski, J. K.; Rulkens, R.; Foucher, D. A.; Lough, A. J.; Macdonald, P. M.; Manners, I. *Macromolecules* **1995**, *28*, 7301.
(7) Rulkens, R.; Lough, A. J.; Manners, I.; Lovelace, S. R.; Grant, C.; Geiger, W. E. *J. Am. Chem. Soc.* **1996**, *118*, 12683.
(8) Rasburn, J.; Petersen, R.; Jahr, T.; Rulkens, R.; Manners, I.; Vancso, J. G. *Chem. Mater.* **1995**, *7*, 871.
(9) Fong, H.; Chun, I.; Reneker, D. H. *Polymer* **1999**, *40*, 4585.
(10) Baumgarten, P. K. *J. Colloid Interface Sci.* **1971**, *36*, 71.
(11) Reneker, D. H.; Chun, I. *Nanotechnology* **1996**, *7*, 215.
(12) Reneker, D. H.; Yarin, A.; Fong, H.; Koombhongse, S. *J. Appl. Phys.* **2000**, *87*, 4531.
(13) Fong, H.; Reneker, D. H. *J. Polym. Sci., Part B: Polym. Phys.* **1999**, *37*, 3488.
(14) Chen, Z.; Foster, M. D. WAXD powder diffraction of the same materials used for creating nanofibers from electrospinning, unpublished work.
(15) Papkov, V. S.; Gerasimov, M. V.; Dubovik, I. I.; Sharma, S.; Dementiev, V. V.; Pannell, K. H. *Macromolecules* **2000**, *33*, 7107.

MA991857N